Loss of STAT3 in murine NK cells enhances NK cell-dependent tumor surveillance

Blood First Edition Paper, prepublished online September 2, 2014; DOI 10.1182/blood-2014-03-564450

Loss of STAT3 in murine NK cells enhances NK cell-dependent tumor surveillance

Dagmar Gotthardt,[1] Eva M. Putz,[1] Elisabeth Straka,[1] Petra Kudweis,[1] Mario Biaggio,[2] Valeria Poli,[3] Birgit Strobl,[2] Mathias Müller,[2] Veronika Sexl[1]

[1]Institute of Pharmacology and Toxicology, Department for Biomedical Sciences, University of Veterinary Medicine Vienna, A-1210 Vienna, Austria

[2]Institute of Animal Breeding and Genetics, Department for Biomedical Sciences, University of Veterinary Medicine Vienna, A-1210 Vienna, Austria

[3]Molecular Biotechnology Center, University of Turin, I-10126 Torino

Running title: STAT3 in NK cell-mediated tumor surveillance

Correspondence

Veronika Sexl

Institute of Pharmacology and Toxicology,

University of Veterinary Medicine Vienna,

Veterinärplatz 1, A-1210 Vienna, Austria

Phone number: 0043 1 25077 2910

Fax: 0043 1 25077 2990

Email: veronika.sexl@vetmeduni.ac.at

Key Points

1. Loss of STAT3 in NK cells enhances the expression of granzyme B, perforin and DNAM-1 resulting in enhanced tumor surveillance
2. STAT3 binds the IFN-γ promoter and interferes with cytokine-induced IFN-γ production in NK cells

Abstract

The members of the STAT family of transcription factors modulate the development and function of NK cells. NK cell-mediated tumor surveillance is particularly important in the body's defense against hematological malignancies such as leukemia. STAT3 inhibitors are currently being developed, although their potential effects on NK cells are not clear. We have investigated the function of STAT3 in NK cells with *Stat3*$^{\Delta/\Delta}$*Ncr1*-iCreTg mice, whose NK cells lack STAT3. In the absence of STAT3, NK cells develop normally and in normal numbers but display alterations in the kinetics of IFN-γ production. We report that STAT3 directly binds the IFN-γ promoter. In various *in vivo* models of hematological diseases loss of STAT3 in NK cells enhances tumor surveillance. The reduced tumor burden is paralleled by increased expression of the activating receptor DNAM-1 and the lytic enzymes perforin and granzyme B. Our findings imply that STAT3 inhibitors will stimulate the cytolytic activity of NK cells against leukemia, thereby providing an additional therapeutic benefit.

Introduction

The JAK/STAT signaling pathway is involved in many cellular processes including development, differentiation and proliferation[1]. STAT transcription factors may induce or repress transcription and have been implicated in NK cell development and function[2–6]. STAT1 is known to regulate NK cell cytotoxicity and cytokine production[5,7]. STAT4 is highly expressed in resting NK cells and regulates IFN-γ production upon IL-12 stimulation by activating the T-box transcription factor T-bet[8,9]. STAT5 is essential for NK cell development and survival mediating IL-2 and IL-15 signaling[10] and STAT6 has been reported to be involved in the differentiation of NK cells[11]. STAT3 is constitutively activated in many cancers and has been reported to mediate the crosstalk between tumor and immune cells[12,13]. Cytokines produced by the tumor activate STAT3 in infiltrating immune cells and suppress their activity[13]. As a consequence NK cell functions may be altered – inhibitory as well as activating effects have been reported[2–4].

Inhibiting STAT3 is a potential approach for the treatment of various forms of cancer. However, our knowledge of the role of STAT3 in NK cells is limited. Kortylewski and colleagues studied *Stat3*$^{\Delta/\Delta}$*Mx1*-Cre mice lacking STAT3 in all Mx1-expressing cells. They reported improved tumor surveillance against B16F10 melanoma cells, which was attributed to T cells and neutrophils. *Stat3*$^{\Delta/\Delta}$*Mx1*-Cre NK cells killed YAC-1 cells better, albeit only after prior B16F10 challenge[14]. The complex interaction of the immune system does not allow any conclusion on the cell-intrinsic role of STAT3 in NK cells.

To assess the role of STAT3 in NK cells we crossed *Stat3*$^{fl/fl}$ with *Ncr1*-iCreTg mice[10,15]. *Stat3*$^{\Delta/\Delta}$*Ncr1*-iCreTg mice lack *Stat3* in the NKp46^{+} NK cell compartment and are viable, fertile and show no obvious signs of disease. The use of *Stat3*$^{\Delta/\Delta}$*Mx1*-Cre mice, where STAT3 is deleted

in all cells including the entire hematopoietic compartment enabled us to compare the phenotype of *Stat3*$^{\Delta/\Delta}$*Ncr1*-iCreTg mice with the consequences of global STAT3 loss.

Material and Methods

Mice

Mice were bred on C57BL/6N background and maintained at the University of Veterinary Medicine Vienna under pathogen-free conditions according to FELASA guidelines. Following mice were studied: *Stat3*$^{fl/fl}$*Mx1*-Cre (inducible Cre expression in all cells that express the Mx1 promoter after type 1 interferon response, e.g. after Poly(I:C) injection, expressing one allele of the Cre-transgene)[16], *Stat3*$^{\Delta/\Delta}$*Ncr1*-iCreTg and *Stat3*$^{fl/fl}$ littermates[15], C57BL/6 mice expressing one allele of the Cre-transgene (*Ncr1*-iCreTg)[10]and wild-type littermates. All experiments were carried out with age-matched 6-12 week old mice and were approved by the institutional ethics committee and conform to Austrian law (license 66.009/0019-II/10b/2010 14.1.10 and 68.205/0218-II/3b/2012).

Cell culture

Splenic NK cells were isolated using DX5-labeled MACS® beads according to the manufacturer's instructions (Miltenyi) and cultured with 5.000U/ml rhIL-2 (Proleukin®, Novartis). NK cell stimulations were performed in the presence of 5.000U/ml rhIL-2 ± 5ng/ml rmIL-12 (R&D), 50ng/ml rmIL-15 (PeproTech), 100U/ml rmIFN-β (Sigma), 5ng/ml rmIL-10 (R&D), 100ng/ml rmIL-21 (Immunotools), 50ng/ml rmIL-23 (R&D), 100ng/ml rmIL-18 (R&D), 50ng/ml rmIL-6 (R&D) or 50ng/ml rmIL6Rα (R&D). Tumor cell lines were cultured as previously published[5]. Both *v-abl*$^{+}$ transformed cell lines used in this study were derived from C57BL6/N mice.

Poly(I:C) treatment

Stat3$^{fl/fl}$ and *Stat3*$^{fl/fl}$*Mx1*-Cre mice were treated three times by i.p. injection of 300µg Poly(I:C) (Sigma) during 14 days. 7 days after the last injection mice were analyzed. Deletion of *Stat3* in *Stat3*$^{fl/fl}$*Mx1*-Cre results in a global *Stat3* deletion in this mouse model including the entire hematopoietic compartment and is denoted as *Stat3*$^{\Delta/\Delta}$*Mx1*-Cre.

NK cell cytotoxicity

In vitro cytotoxicity assays were performed as previously published[5,17]. For the DNAM-1 blockade, NK cells were incubated with anti-CD226 for 1 hour at 4°C and washed. Blocking efficiency was checked by flow cytometry and the blocked cells were incubated with the tumor cells at different E:T ratios.

***In vivo* tumor challenge**

For the B16F10 melanoma model, mice were injected i.v. with $5x10^4$ B16F10 cells. After 24 days mice were sacrificed and lung tissue analyzed. Tumor nodules in the lung were counted by three independent researchers in a blinded manner. During the disease progression blood was analyzed by flow cytometry. For Kaplan-Meier plots, mice were sacrificed at the first signs of dyspnea and health detractions.

In the *v-abl* leukemic tumor model, 10^6 *v-abl*$^+$ tumor cells were injected i.v. or s.c. into each flank of the mice. After s.c. injection, mice were sacrificed at day 12 and tumor weight was determined. For the survival assay (i.v. injection), mice were sacrificed at first signs of paralysis and health detractions. During the disease progression the blood was analyzed by flow cytometry.

In the A-MuLV model newborn mice were injected with 100µL of replication-incompetent

ecotropic retrovirus encoding for *v-abl* by i.p. injection as described previously[18]. Mice were checked daily for disease onset.

Western blotting

Preparation of protein lysates and western blot was done as previously reported[5]. Following antibodies were used: STAT3 (Cell Signaling CS#9132), pSTAT3-Y705 (CS#9131), STAT4 (CS#2653), pSTAT4-Y693 (BD-612738), pSTAT5-Y694 (BD-611964), STAT5 (sc-836) (Santa Cruz), Granzyme B (CS#4275), Perforin (CS#3693) and ß-actin (sc-69879). Immunoreactive bands were visualized by chemiluminescence detection (LumiGLO®, Cell Signaling) by the ChemiDoc MP Imaging System (Bio-Rad).

STAT3 Inhibitors

STAT3 Inhibitor VI, S31-201-Calbiochem (#573130) and STAT3 Inhibitor XIV, LLL12-Calbiochem (#573131) were purchased from Merck Millipore. NK cells were treated for 4 hours with inhibitors at the concentration indicated or with DMSO control prior to stimulation with the respective cytokines.

Chromatin Immunoprecipitation (ChIP)

MACS-purified and IL-2 cultured NK cells (10^7) were either left untreated or stimulated with IL-12 for 30 minutes followed by cross-linking using 1% formaldehyde for 10 min at 37 °C. The reaction was stopped by the addition of 0.5M glycine for 5 min. Cell nuclei were prepared and lysed in 1ml of lysis buffer on 4°C o/n. Chromatin was sheared by sonication yielding chromatin fragments between 100-500bp and diluted 2.5-fold in ChIP dilution buffer. IPs were performed at 4°C o/n with an anti-STAT3 antibody (Cell Signaling CS#9132). Chromatin was pre-cleared using 25µl salmon sperm DNA/protein A-agarose beads and incubated with the antibody o/n.

Immune complexes were collected with 25µl beads for 3 hours and washed with RIPA buffer, high salt buffer, LiCl buffer and TE buffer. Samples were eluted 2x in elution buffer (2% SDS, 10mM DTT and 100mM $NaHCO_3$). DNA cross-linking was reversed by heating at 65 °C o/n followed by proteinase K digestion. DNA was extracted with phenol-chloroform, precipitated in isopropanol and resuspended in TE Buffer. The predicted binding site was obtained using Ensemble for the sequence of the IFN-γ promoter and blasting for the potential STAT binding motif $TTC(N)_{2\text{-}4}GAA$ (Figure S4F). Obtained DNA fragments were analyzed by qPCR using the following primer pairs: *Ifng*: Fw:5'-GTGCTGTGCTCTGTGGATGAG-3'and Rev:5'-GAAGGCTCCTCGGGATTACGT-3' $CD19^{down}$: Fw:5'-CCCTCTTCTCATTCGTTTTCCA-3'and Rev:5'-CCAGGAAAGAATTTGAGAAAAATCA -3'. N-fold enrichment was calculated relative to a negative region downstream of the CD19 gene ($CD19^{down}$).

Histology

Paraffin-embedded sections (3µm) were stained with Hematoxylin/Eosin according to standard histological procedures. Blood smears were fixated and stained using Hemacolor® staining kit (Merck). All stainings were scanned and photographed with an Olympus IX71 microscope using CellSens Dimension Software (Olympus).

Statistical analysis

Unpaired *t*-test, Mann-Whitney (non-parametrical), one-way ANOVA with Tukey's post hoc test and log-rank tests were performed using GraphPad Prism® Software version 5.0 (San Diego California USA) where appropriate. The level of significance is indicated for each experiment (* $p < 0.05$; ** $p < 0.01$; *** $p < 0.001$).

Results

NK cells develop and mature normally in the absence of *Stat3*

The numbers of NK cells in spleen and bone marrow were comparable in *Stat3*$^{\Delta/\Delta}$*Mx1*-Cre (where STAT3 is absent from the entire hematopoietic compartment) and *Stat3*$^{\Delta/\Delta}$*Ncr1*-iCreTg mice (lacking STAT3 only in the NKp46^{+} NK cell compartment) and their *Stat3*$^{fl/fl}$ littermates (Figure 1A+C, S1A-B). NK cells differentiate from NK Precursors (NKP) to immature NK cells (iNK) before becoming fully mature (mNK) and migrating to the periphery[19]. NK cells at all stages of development (a gating scheme is presented in Figure 1B) are present at comparable numbers in *Stat3*$^{\Delta/\Delta}$*Ncr1*-iCreTg mice (Figure 1C, S1B). In *Stat3*$^{\Delta/\Delta}$*Mx1*-Cre animals we detected an increase in the NKP population, which does not translate to altered numbers of mature NK cells but most likely reflects changes in the cytokine milieu in the bone marrow of these animals (Figure S1B). Q-PCR analysis verified the successful deletion and the significant decrease in levels of Stat3 mRNA (Figure 1D). While NK cells develop in the bone marrow, NK cell maturation occurs in the spleen. We failed to detect any significant changes in NK cell maturation in *Stat3*$^{\Delta/\Delta}$*Ncr1*-iCreTg and *Stat3*$^{\Delta/\Delta}$*Mx1*-Cre mice compared to their *Stat3*$^{fl/fl}$ littermates (Figure 1E-F and S1F-G). Similarly, when we expanded NK cells derived from *Stat3*$^{\Delta/\Delta}$*Ncr1*-iCreTg mice and *Stat3*$^{fl/fl}$ controls *in vitro*, no alterations in cell growth or cell cycle distribution were detected (Figure S1H). Confirmation that NK cell proliferation is not altered came from *in vivo* BrdU incorporation experiments; BrdU incorporation in splenic and bone marrow NK cells was comparable (Figure S1I). In summary, the data led us to conclude that STAT3 is not required for survival, proliferation or development of NK cells.

NK cells bind their target cells via specific receptors. By integrating signals from activating and inhibitory receptors, NK cells ultimately lyse a target cell or leave it unaffected. Levels of

CD122, of the activating receptors NKp46, NKG2C/E, NKG2D, 2B4, Ly49D and H and of the inhibitory receptors KLRG1, NKG2A, Ly49A,C,G2 and I are superimposable in *Stat3*$^{fl/fl}$, *Stat3*$^{\Delta/\Delta}$*Ncr1*-iCreTg and *Stat3*$^{\Delta/\Delta}$*Mx1*-Cre splenic NK cells (Figure 1G and S1C). However, loss of STAT3 is associated with a consistently and significantly increased number of NK cells expressing the activating receptor DNAM-1 (CD226) (Figure 1G, S1D), which suppresses tumors by binding its ligands CD155 and CD112 on target cells[20,21]. The enhanced expression of DNAM-1 in the absence of STAT3 was confirmed in NK cells derived from *Stat3*$^{\Delta/\Delta}$*Mx1*-Cre mice (Figure S1C+E).

Cytokine stimulation in splenic and intestinal NKp46$^+$ cells

We next investigated which cytokines induce STAT3 activation in primary (Figure 2A) and IL-2 expanded NK cells (Figure 2B). IL-2 treatment is required to keep the cells viable. It induces STAT3-Y705 phosphorylation that is further increased upon stimulation with IL-10, IL-12, IL-15 or IFN-ß (Figure 2A). In contrast, in IL-2 cultured NK cells stimulation with IL-15 fails to induce STAT3 phosphorylation. Remarkably, IL-21 was able to provoke a strong pSTAT3 response under these experimental conditions (Figure 2B).

IL-23 fails to trigger activation of STAT3 in splenic NK cells but this does not necessarily imply that the IL-23-induced IL-22 production[22] in intestinal NKp46$^+$ ILC3 cells is independent of STAT3. To clarify this point, we stimulated lamina propria cells of the small intestine and colon of *Stat3*$^{fl/fl}$ and *Stat3*$^{\Delta/\Delta}$*Ncr1*-iCreTg animals with IL-23. No changes in the numbers of intestinal NKp46$^+$ or NKp46$^+$ IL-22$^+$ cells were detectable (Figure 2C).

To investigate whether the increase in DNAM-1$^+$ NK cells is regulated by a distinct cytokine, we stimulated splenocytes of *Stat3*$^{fl/fl}$ and *Stat3*$^{\Delta/\Delta}$*Ncr1*-iCreTg mice with various cytokines as

indicated. No changes were observed - significantly more *Stat3*$^{\Delta/\Delta}$*Ncr1*-iCreTg NK cells expressed DNAM-1 (Figure S2A). Under identical experimental conditions we uncovered a slight decrease of IFN-γ expression in cells lacking STAT3 irrespective of the stimulus (Figure S2B), while perforin levels were elevated upon stimulation with IL-2, IL-15, IL-12 /IL-15, IL-21 and IFN-β (Figure S2C). Numbers of granzyme B^{+} cells were only slightly increased after combined stimulation with IL-12 and IL-15 (Figure S2D). This finding prompted us to investigate the production of perforin, granzyme B and IFN- γ in more detail.

Increased levels of perforin and granzyme B in the absence or upon inhibition of STAT3

Levels of granzyme B protein and mRNA were investigated using freshly purified NK cells of *Stat3*$^{fl/fl}$, *Stat3*$^{\Delta/\Delta}$*Ncr1*-iCreTg NK cells (Figure 3A+C) and *Stat3*$^{\Delta/\Delta}$*Mx1*-Cre NK cells (Figure 3B). Interestingly, despite elevated protein levels granzyme B mRNA was unaltered under comparable experimental conditions (Figure 3C). In contrast, we readily detected increased levels of perforin mRNA expression upon stimulation with IL-2 and IL-12 (Figure 3C). Intracellular FACS staining verified that the levels of perforin and granzyme B were significantly enhanced in cells derived from *Stat3*$^{\Delta/\Delta}$*Ncr1*-iCreTg mice, both in non-stimulated NK cells *ex vivo* as well when the cell were stimulated with IL-2, IL-12 and IL-15 (Figure 3D-E). In contrast, levels of granzyme A remained unaffected by loss of STAT3 (Figure S3A-B).

STAT3 inhibitors are currently being developed and hold great promise for the treatment of cancer. We tested the effects of inhibitors LLL-12 and S31-201 on levels of perforin and granzyme B in primary NK cells. At concentrations where the inhibitors efficiently block STAT3 activation (Figure 3F), they induced increased levels of perforin mRNA upon IL-2/IL-12/IL-15 treatment. The effects on granzyme B mRNA were not consistent in line with the unaltered mRNA regulation upon *Stat3* deletion (Figure 3G).

NK cells lacking *Stat3* show altered kinetics of IFN-γ production

STAT3 is involved in the response to and the secretion of cytokines[13,23,24].Intracellular FACS staining revealed a decrease in IFN-γ expression after 4 hours of IL-12 stimulation in *Stat3* deficient NK cells. Interestingly, after stimulation for 8 hours the difference disappeared (Figure 4A-B). Regulation of IFN-γ production is complex and involves the transcriptional regulator T-bet[8,9]. Intracellular FACS staining showed unaltered levels of T-bet after 4 hours of IL-12 stimulation despite the reduction of IFN-γ^+ NK cells in *Stat3*$^{\Delta/\Delta}$*Ncr1*-iCreTg and in *Stat3*$^{\Delta/\Delta}$*Mx1*-Cre mice (Figure 4A and S4B-D). Similarly, expression of IL-12 receptor was unaltered (Figure S4E). IFN-γ production is also controlled by members of the STAT family and STAT4 has a key role in IL-12 induced production of IFN-γ[25]. It is thus conceivable that STAT3 binds the IFN-γ promoter and interferes with STAT–driven transcription. Chromatin Immunoprecipitation (ChIP) assays in primary NK cells indeed showed that IL-12 induced binding of STAT3 to the IFN-γ promoter (Figure 4C) with binding occurring at a STAT binding region illustrated in Figure S4F[26]. Absence of STAT3 may also alter the activation of other members of the STAT family: Levels of pSTAT4 and pSTAT5 were enhanced in *ex vivo*-derived *Stat3*$^{\Delta/\Delta}$*Ncr1*-iCreTg NK cells (Figure 4D).

We used an anti-NK1.1 antibody to investigate whether changes in IFN-γ production also occur upon receptor stimulation. We failed to detect any significant differences in secretion of IFN-γ secretion between *Stat3*$^{fl/fl}$ and *Stat3*$^{\Delta/\Delta}$*Ncr1*-iCreTg NK cells (Figure 4E) and no significant alterations in the production of IFN-γ by Ly49C$^{-/+}$ NK cells were found (Figure 4F+S4A). These experiments indicate that STAT3 contributes to IFN-γ production upon IL-12 stimulation although it is of minor importance upon NK cell receptor stimulation.

Enhanced NK cell-dependent tumor surveillance in the absence of STAT3

We next asked whether the enhanced levels of perforin, granzyme B and DNAM-1 in *Stat3*$^{fl/fl}$ and *Stat3*$^{\Delta/\Delta}$*Ncr1*-iCreTg mice result in an enhanced NK cell-mediated tumor surveillance. We used B16F10 cells, a well-established tumor model controlled by NK cells[10,27,28]. B16F10 cells were injected i.v. and tumor burden was analyzed after three weeks. Disease latency was significantly enhanced and accompanied by a drastic reduction of tumor nodules on day 24 in *Stat3*$^{\Delta/\Delta}$*Ncr1*-iCreTg mice (Figure 5A-B, S5A). B16F10 induced tumor formation was even more suppressed in *Stat3*$^{\Delta/\Delta}$*Mx1*-Cre mice, although deletion of STAT3 in the NK cell compartment alone largely sufficed to improve tumor surveillance (Figure S5D). The improved tumor surveillance was accompanied by consistently elevated numbers of DNAM-1^{+} NK cells in the blood (Figure 5C), whereas the levels of CMKLR1 recognizing the chemoattractant chemerin and the exhaustion marker PD-1 were unaltered (Figure S5B-C). Consistently, *in vitro* cytotoxicity assays showed that the melanoma cell line B16F10 was killed more efficiently by NK cells lacking STAT3 (Figure 5D). No differences were observed in cytotoxicity assays using other target cell lines. One major difference between target cell lines is the expression of the DNAM-1 ligand CD155, which is only found at high levels in B16F10 cells (Figure 5E). Blocking DNAM-1 using antibodies significantly reduced cytotoxicity and abolished the differences between *Stat3*$^{\Delta/\Delta}$*Ncr1*-iCreTg and control cells (Figure 5F). Cytotoxicity against other target cell lines depends on other recognition receptors, activation of which ultimately leads to the release of granzymes and perforin. *In vitro* cytotoxicity assays employ NK cells expanded in IL-2 for a week. Western blot experiments showed that the changes in levels of perforin and granzyme B that we observe in freshly isolated NK cells lacking STAT3 are no longer detectable upon cultivation with IL-2 (Figure S5E) whereas the differences related to an increase in % DNAM-1^{+} cells persist (Figure S5F).

Loss of STAT3 in NK cells improves tumor surveillance against leukemia

An increasing body of evidence describes control of leukemogenesis in an NK cell-dependent manner[29–31]. We used the well-established Bcr/Abl leukemia model to test the effect of deleting STAT3. We subcutaneously injected *v-abl*$^{+}$ leukemic cell lines into *Stat3*$^{fl/fl}$ and *Stat3*$^{\Delta/\Delta}$*Ncr1*-iCreTg mice. Twelve days later large tumors had evolved in *Stat3*$^{fl/fl}$ animals whereas a pronounced reduction of tumor mass was observed in *Stat3*$^{\Delta/\Delta}$*Ncr1*-iCreTg mice (Figure 6A-B). Further evidence that the absence of STAT3 in the NK cell compartment significantly enhances NK cell-mediated tumor surveillance was obtained by injecting two individually derived leukemic cell lines intravenously into *Stat3*$^{fl/fl}$ and *Stat3*$^{\Delta/\Delta}$*Ncr1*-iCreTg mice (Figure 6C, S6A). Again, *Stat3*$^{\Delta/\Delta}$*Ncr1*-iCreTg animals survived significantly longer than the control animals. Finally we injected newborn mice with a replication-incompetent ecotropic retrovirus encoding for *v-abl*. This model system more closely mimics the development of human disease: a mono- or oligoclonal disease evolves slowly and is under the tight control of NK cells[31]. Again, disease incidence and disease latency differed significantly. Whereas all *Stat3*$^{fl/fl}$ mice and control mice expressing only Cre recombinase succumbed to disease, 20% of *Stat3*$^{\Delta/\Delta}$*Ncr1*-iCreTg mice survived and disease latency was significantly delayed (Figure 6D and S6B). There were no visible differences in the phenotype of the disease and all mice were densely infiltrated with leukemic cells at the end stage of disease (Figure 6E). We also detected constantly increased numbers of DNAM-1^{+} NK cells in the blood of *Stat3*$^{\Delta/\Delta}$*Ncr1*-iCreTg mice during disease progression (Figure S6C).

Discussion

We report a pronounced suppressive effect of STAT3 on NK cell-mediated tumor surveillance. In the absence of STAT3, murine NK cells develop and mature normally. Challenging the mice with tumor cells uncovered the key role of STAT3 in NK cell-mediated tumor surveillance. Experiments with the B16F10 melanoma model revealed a significantly delayed tumor formation in *Stat3*$^{\Delta/\Delta}$*Ncr1*-iCreTg mice. The improved tumor cell rejection extends to hematopoietic malignancies: *Bcr/Abl*$^{+}$ leukemic cell lines are significantly better controlled by *Stat3*-deficient NK cells irrespective of the experimental model used. Most importantly, work with a slowly evolving mono- or oligoclonal leukemia provoked by the injection of a retrovirus encoding A-MuLV – which closely resembles the development of human disease – confirmed the significant delay in tumorigenesis in *Stat3*$^{\Delta/\Delta}$*Ncr1*-iCreTg mice animals. The experiments illustrate the power and significance of NK cell-mediated tumor surveillance and reveal that STAT3 has a tumor promoting role in NK cells. NK cells lacking STAT3 are significantly better equipped to eliminate tumor targets.

Hua Yu and Kortylewski were the first to show that deletion of STAT3 in the hematopoietic compartment improves tumor immune surveillance[14]. The comparison of B16F10-dependent tumor cell rejection in *Stat3*$^{\Delta/\Delta}$*Ncr1*-iCreTg and *Stat3*$^{\Delta/\Delta}$*Mx1*-Cre mice confirms the effect of *Stat3* deletion in the NK cell compartment. Although tumor surveillance is further improved in *Stat3*$^{\Delta/\Delta}$*Mx1*-Cre mice, a substantial portion of the beneficial effect stems from deletion of *Stat3* in NK cells.

NK cells are important producers of IFN-γ, which is a critical determinant of tumor surveillance. We discovered that STAT3 regulates IFN-γ production by binding the IFN-γ promoter upon IL-12 stimulation. In the absence of STAT3, the onset of IFN-γ secretion upon cytokine stimulation

is delayed. However, the changed kinetics does not translate to impaired tumor surveillance. It is attractive to speculate that other members of the STAT transcription factor family compensate for the absence of STAT3.

In the absence of STAT3 there is a consistent increase in levels of perforin and granzyme B in NK cells. The difference is abrogated upon cultivation in IL-2. As perforin is a target of STAT5[32,33], it is likely that the persistent strong IL-2 stimulation that triggers STAT5 activation blurs the differences observed in freshly isolated cells. As a consequence, studies of cytotoxicity *in vivo* and *in vitro* give different results. The level of perforin is an important determinant of NK cell cytotoxicity and NK cells lacking one allele of perforin have an impaired capacity to kill[34]. The comparable levels of perforin and granzyme B in *Stat3*-deficient NK cells maintained in culture explain why the NK cell-dependent cytotoxicity against hematopoietic tumor cell lines *in vitro* are superimposable with those of wild-type NK cells. *In vivo*, where perforin and granzyme B are increased in *Stat3*$^{\Delta/\Delta}$*Ncr1*-iCreTg mice, NK cell-dependent tumor surveillance is clearly enhanced. Differences in NK cell-dependent cytotoxicity are only seen *in vitro* when target cells express DNAM-1 ligands at high levels. In contrast to perforin, %DNAM-1$^+$ cells remain elevated in *Stat3*-deficient NK cells even upon prolonged culture *in vitro*[21]. Recent evidence links DNAM-1 to perforin: DNAM-1 is required for IL-2-activated perforin-mediated antitumor responses[20]. There is a need for caution when comparing *in vitro* and *in vivo* data, as prolonged culture of NK cells in IL-2 changes intracellular signaling patterns and consequently gene expression.

The increased numbers of DNAM-1$^+$ NK cells are accompanied by elevated levels of perforin and granzyme B, which may contribute to the enhanced NK cell-mediated tumor cell killing. To date there are no reports on gene dosage effects regarding granzyme B, although it has been

suggested that altered granzyme B expression contributes to increased tumor cell surveillance[35,36]. Interestingly, the amount of granzyme B protein was increased without a concomitant change in the level of mRNA, suggesting the involvement of microRNAs. Both perforin and granzyme B have been described as targets of microRNA-dependent regulation in NK cells[37–39]. Further research will be required to investigate whether STAT3 interferes with the control of microRNAs in NK cells.

In summary, our *in vivo* data define an inhibitory role for STAT3 in NK cell-dependent tumor surveillance. The evidence is compelling and unambiguous. The increase in cytolytic capacity involves more than one downstream molecular target; the increased expression levels of DNAM-1, perforin and granzyme B contribute to the effect. Our conclusions are based on several independent tumor models and it appears likely that they will be relevant to additional systems, including human cancers. The mechanism is still not fully understood and we cannot exclude the possibility that other mechanisms are involved. Further research is required to discover which molecular players contribute to the *in vivo* effects of deleting STAT3 in the NK cell compartment.

Our observations improve the prospects of patients suffering from cancer controlled by NK cell-dependent surveillance, such as many hematological diseases. Recent evidence has highlighted the contribution of NK cells to the control of minimal residual disease[40]. Although STAT3 has a dual role in tumor formation and acts both as a tumor suppressor and as a tumor promoter, in hematological malignancies it functions predominantly as tumor promoter. Mutations in STAT3 have been proposed to be drivers of hematological disorders[41,42] and inhibitors of STAT3 are being developed as novel anti-cancer therapeutics[43–45]. Although we are unaware of any STAT3 inhibitors that have entered clinical trials, clinical use is expected in the near future. Our study

shows that inhibiting STAT3 in NK cells will not only affect the tumor cells themselves but will have the additional benefit of improving tumor surveillance.

Leukemia and melanoma are among the types of cancer known to be controlled by NK cells. In planning tumor therapy, it is therefore important to consider the beneficial effects of STAT3 inhibitors on NK cell-mediated tumor surveillance – it may be possible to kill two birds with one stone.

Acknowledgments

We want to thank G. Tebb, S. Fajmann, P. Jodl and Z. Horvath-Bago for their help. We are grateful to the mouse facility. The work was supported by the FWF grant SFB F28 (to M.M., B.S. and V.S.; http://www.fwf.ac.at/en/projects/sfb.html) and the Herzfelder'sche Familienstiftung (to V.S.).

Authorship

Contribution: D.G., E.M.P., E.S., P.K. and M.B. performed the research, D.G., E.M.P.; B.S., M.M. and V.S. designed the research and analyzed data, V.P. provided reagents; V.S. and D.G. wrote the manuscript.

Conflict of interest disclosure

The authors declare no competing financial interests.

References

1. Horvath CM. STAT proteins and transcriptional responses to extracellular signals. *Trends Biochem. Sci*. 2000;25(10):496–502.

2. Putz EM, Hoelzl MA, Baeck J, et al. Loss of STAT3 in Lymphoma Relaxes NK Cell-Mediated Tumor Surveillance. *Cancers (Basel)*. 2014;6(1):193–210.

3. Bedel R, Thiery-Vuillemin A, Grandclement C, et al. Novel role for STAT3 in transcriptional regulation of NK immune cell targeting receptor MICA on cancer cells. *Cancer Res.* 2011;71:1615–1626.

4. Sun X, Sui Q, Zhang C, Tian Z, Zhang J. Targeting blockage of STAT3 in hepatocellular carcinoma cells augments NK cell functions via reverse hepatocellular carcinoma-induced immune suppression. *Mol. Cancer Ther.* 2013;12(12):2885–96.

5. Putz EM, Gotthardt D, Hoermann G, et al. CDK8-Mediated STAT1-S727 Phosphorylation Restrains NK Cell Cytotoxicity and Tumor Surveillance. *Cell Rep.* 2013;1–8.

6. Ecker A, Simma O, Hoelbl A, et al. The dark and the bright side of Stat3: proto-oncogene and tumor-suppressor. *Front. Biosci. (Landmark Ed.)* 2009;14:2944–58.

7. Lee CK, Rao DT, Gertner R, et al. Distinct requirements for IFNs and STAT1 in NK cell function. *J Immunol*. 2000;165(7):3571–3577.

8. Miyagi T, Gil MP, Wang X, et al. High basal STAT4 balanced by STAT1 induction to control type 1 interferon effects in natural killer cells. *J Exp Med*. 2007;204(10):2383–2396.

9. Townsend MJ, Weinmann AS, Matsuda JL, et al. T-bet regulates the terminal maturation and homeostasis of NK and Valpha14i NKT cells. *Immunity*. 2004;20(4):477–494.

10. Eckelhart E, Warsch W, Zebedin E, et al. A novel Ncr1-Cre mouse reveals the essential role of STAT5 for NK-cell survival and development. *Blood*. 2011;117(5):1565–73.

11. Katsumoto T, Kimura M, Yamashita M, et al. STAT6-dependent differentiation and production of IL-5 and IL-13 in murine NK2 cells. *J Immunol*. 2004;173(8):4967–75.

12. Yu H, Jove R. The STATs of cancer--new molecular targets come of age. *Nat. Rev. Cancer*. 2004;4:97–105.

13. Yu H, Kortylewski M, Pardoll D. Crosstalk between cancer and immune cells: role of STAT3 in the tumour microenvironment. *Nat. Rev. Immunol.* 2007;7(1):41–51.

14. Kortylewski M, Kujawski M, Wang T, et al. Inhibiting Stat3 signaling in the hematopoietic system elicits multicomponent antitumor immunity. *Nat. Med.* 2005;11(12):1314–1321.

15. Alonzi T, Maritano D, Gorgoni B, et al. Essential role of STAT3 in the control of the acute-phase response as revealed by inducible gene inactivation [correction of activation] in the liver. *Mol Cell Biol*. 2001;21(5):1621–1632.

16. Kuhn R, Schwenk F, Aguet M, Rajewsky K. Inducible gene targeting in mice. *Science.* 1995;269:1427–1429.

17. Mizutani T, Neugebauer N, Putz EM, et al. Conditional IFNAR1 ablation reveals distinct requirements of Type I IFN signaling for NK cell maturation and tumor surveillance. *Oncoimmunology*. 2012;1(7):1027–1037.

18. Sexl V, Piekorz R, Moriggl R, et al. Stat5a/b contribute to interleukin 7-induced B-cell precursor expansion, but abl- and bcr/abl-induced transformation are independent of Stat5. *Blood*. 2000;96:2277–2283.

19. Kim S, Iizuka K, Kang H-SPS, et al. In vivo developmental stages in murine natural killer cell maturation. *Nat Immunol*. 2002;3(6):523–528.

20. Chan CJ, Andrews DM, McLaughlin NM, et al. DNAM-1/CD155 interactions promote cytokine and NK cell-mediated suppression of poorly immunogenic melanoma metastases. *J Immunol*. 2010;184(2):902–11.

21. Lakshmikanth T, Burke S, Ali TH, et al. NCRs and DNAM-1 mediate NK cell recognition and lysis of human and mouse melanoma cell lines in vitro and in vivo. *J. Clin. Invest.* 2009;119:1251–1263.

22. Sanos SL, Bui VL, Mortha A, et al. RORgammat and commensal microflora are required for the differentiation of mucosal interleukin 22-producing NKp46+ cells. *Nat. Immunol.* 2009;10(1):83–91.

23. Yang XO, Panopoulos AD, Nurieva R, et al. STAT3 regulates cytokine-mediated generation of inflammatory helper T cells. *J. Biol. Chem.* 2007;282(13):9358–63.

24. Harris TJ, Grosso JF, Yen H, et al. Development and T H 17-Dependent Autoimmunity 1. *J Immunol*. 2007;179:1–5.

25. Xu X, Sun YL, Hoey T. Cooperative DNA binding and sequence-selective recognition conferred by the STAT amino-terminal domain. *Science*. 1996;273:794–797.

26. Nguyen KB, Watford WT, Salomon R, et al. Critical role for STAT4 activation by type 1 interferons in the interferon-gamma response to viral infection. *Science*. 2002;297(5589):2063–6.

27. Grundy MA, Zhang T, Sentman CL. NK cells rapidly remove B16F10 tumor cells in a perforin and interferon-gamma independent manner in vivo. *Cancer Immunol Immunother*. 2007;56(8):1153–1161.

28. Seaman WE, Sleisenger M, Eriksson E, Koo GC. Depletion of natural killer cells in mice by monoclonal antibody to NK-1.1. Reduction in host defense against malignancy without loss of cellular or humoral immunity. *J Immunol*. 1987;138(12):4539–4544.

29. Sanchez-Correa B, Gayoso I, Bergua JM, et al. Decreased expression of DNAM-1 on NK cells from acute myeloid leukemia patients. *Immunol Cell Biol*. 2012;90(1):109–115.

30. Croxford JL, Tang MLF, Pan MF, et al. ATM-dependent spontaneous regression of early Eμ-myc-induced murine B-cell leukemia depends on natural killer and T cells. *Blood*. 2013;121(13):2512–21.

31. Stoiber D, Kovacic B, Schuster C, et al. TYK2 is a key regulator of the surveillance of B lymphoid tumors. *J. Clin. Invest.* 2004;114(11):1650–1658.

32. Yu CR, Ortaldo JR, Curiel RE, et al. Role of a STAT binding site in the regulation of the human perforin promoter. *J Immunol*. 1999;162(5):2785–2790.

33. Zhang J, Scordi I, Smyth MJ, Lichtenheld MG. Interleukin 2 receptor signaling regulates the perforin gene through signal transducer and activator of transcription (Stat)5 activation of two enhancers. *J. Exp. Med.* 1999;190:1297–1308.

34. Lowin B, Beermann F, Schmidt A, Tschopp J. A null mutation in the perforin gene impairs cytolytic T lymphocyte- and natural killer cell-mediated cytotoxicity. *Proc. Natl. Acad. Sci.* 1994;91:11571–11575.

35. Grossman WJ, Verbsky JW, Tollefsen BL, et al. Differential expression of granzymes A and B in human cytotoxic lymphocyte subsets and T regulatory cells. *Blood*. 2004;104(9):2840–8.

36. Oberoi P, Jabulowsky R a, Bähr-Mahmud H, Wels WS. EGFR-targeted granzyme B expressed in NK cells enhances natural cytotoxicity and mediates specific killing of tumor cells. *PLoS One*. 2013;8(4):e61267.

37. Fehniger TA, Wylie T, Germino E, et al. Next-generation sequencing identifies the natural killer cell microRNA transcriptome. *Genome Res.* 2010;20:1590–1604.

38. Kim TD, Lee SU, Yun S, et al. Human microRNA-27a*targets Prf1 and GzmB expression to regulate NK-cell cytotoxicity. *Blood*. 2011;118:5476–5486.

39. Wang P, Gu Y, Zhang Q, et al. Identification of resting and type I IFN-activated human NK cell miRNomes reveals microRNA-378 and microRNA-30e as negative regulators of NK cell cytotoxicity. *J. Immunol.* 2012;189:211–21.

40. Yoshimoto T, Mizoguchi I, Katagiri S, et al. Immunosurveillance markers may predict patients who can discontinue imatinib therapy without relapse. *Oncoimmunology*. 2014;3:e28861.

41. Koskela HLM, Eldfors S, Ellonen P, et al. Somatic STAT3 mutations in large granular lymphocytic leukemia. *N. Engl. J. Med.* 2012;366:1905–13.

42. Rajala HLM, Porkka K, Maciejewski JP, Loughran TP, Mustjoki S. Uncovering the pathogenesis of large granular lymphocytic leukemia-novel STAT3 and STAT5b mutations. *Ann. Med.* 2014;2:1–9.

43. Haftchenary S, Luchman HA, Jouk AO, et al. Potent targeting of the STAT3 protein in brain cancer stem cells: A promising route for treating glioblastoma. *ACS Med. Chem. Lett.* 2013;4:1102–1107.

44. Furqan M, Akinleye A, Mukhi N, et al. STAT inhibitors for cancer therapy. *J. Hematol. Oncol.* 2013;6:90.

45. Munoz J, Dhillon N, Janku F, Watowich SS, Hong DS. STAT3 inhibitors: finding a home in lymphoma and leukemia. *Oncologist*. 2014;19(5):536–44.

Figure Legends

Figure 1: **Lack of STAT3 does not influence NK cell development, maturation and proliferation. (A)** Bar graphs depict absolute numbers of splenic NK cells ($CD3^-$ $NK1.1^+NKp46^+$) of *Stat3*$^{\Delta/\Delta}$*Ncr1*-iCreTg mice and *Stat3*$^{fl/fl}$ controls as determined by flow cytometry. 5 independently conducted experiments with n≥14 per genotype are pooled. Data represent means±SEM. (B) Flow cytometric gating scheme for identification of NKP, iNKs and mNKs in the bone marrow. (C) For the analysis of NK cell development, BM cells of *Stat3*$^{\Delta/\Delta}$*Ncr1*-iCreTg mice and *Stat3*$^{fl/fl}$ controls were counted and analyzed via flow cytometry by gating on Lin^- (CD3, CD19, Ter119, Ly6C/G) $CD122^+$ cells. NK Precursors (NKPs) are defined as $Lin^-CD122^+NK1.1^-DX5^-$, immature NKs (iNKs) as $Lin^-CD122^+NK1.1^+DX5^-$ and mature NKs (mNKs) as $Lin^-CD122^+NK1.1^+DX5^+$. Bar graphs depict means±SEM (n≥6 per genotype). (D) *Stat3* deletion efficiency of MACS-purified NK cells was analyzed *ex vivo* by qPCR. Data represent means±SEM (three replicates per group); gene expression is calculated relative to the housekeeping gene (HKG) *Gapdh* and normalized to *Stat3*$^{fl/fl}$. (E+F) For detection of NK cell maturation stages, splenocytes of *Stat3*$^{fl/fl}$ and *Stat3*$^{\Delta/\Delta}$*Ncr1*-iCreTg mice were analyzed for CD27 and CD11b expression after previous gating on $CD3^-NK.1.1^+$ cells Statistical analyses are summarized in (F) (n≥8 per genotype). (G) Splenocytes of *Stat3*$^{fl/fl}$ and *Stat3*$^{\Delta/\Delta}$*Ncr1*-iCreTg mice

were stained for individual NK cell receptors after gating on NK cells ($CD3^-NK1.1^+$). One representative histogram is shown (4 independent experiments, with n≥10 in total per genotype). There are significantly more *Stat3*$^{\Delta/\Delta}$*Ncr1*-iCreTg NK cells expressing DNAM-1: 57±0.8 (*Stat3*$^{fl/fl}$) vs. 66±1.5 (*Stat3*$^{\Delta/\Delta}$*Ncr1*-iCreTg) %DNAM-1^+ NK cells. Statistics are included into Figure S1D.

Figure 2: **Different cytokines activate STAT3 in primary and IL-2 expanded NK cells**. (A) NK cells were MACS-purified, FACS-sorted and stimulated with IL-2 alone or together with IL-6 (+IL6Rα), IL-10, IL-12, IL-15, IL-18, IL-21, IL-23 or IFN-ß for 20 minutes. Western blot analysis show levels of pSTAT3-Y705 and STAT3. ß-actin was detected as loading control. (B) IL-2 expanded NK cells were stimulated with indicated cytokines for 20 or 200 minutes. Western blots show levels of pSTAT3-Y705 and STAT3. ß-actin was used as loading control. (C) Lamina propria cells from the colon or small intestine of *Stat3*$^{fl/fl}$ *and Stat3*$^{\Delta/\Delta}$*Ncr1*-iCreTg mice. Cells were stimulated with IL-23, fixed and permeabilized and IL-22 production of $CD45^+CD3^-CD19^-$ $NKp46^+$ cells was analyzed by flow cytometry.

Figure 3: **Loss of STAT3 in NK cells is accompanied by increased expression of perforin and granzyme B**. (A+B) One representative Western blot (n=2) of (A) *ex vivo* MACS-purified and $CD3^-NKp46^+$ sorted *Stat3*$^{fl/fl}$ and *Stat3*$^{\Delta/\Delta}$*Ncr1*-iCreTg NK cells and (B) MACS-purified and IL-2 expanded *Stat3*$^{fl/fl}$ and *Stat3*$^{\Delta/\Delta}$*Mx1*-Cre NK cells without any stimulus or after stimulation for 30 minutes with IL-2+IL-12, 3 hours with IL-2+IL-12 or 30 minutes with IL-2+IL-15. STAT3 activation, STAT3 deletion in *Stat3*$^{\Delta/\Delta}$*Ncr1*-iCreTg NK cells and granzyme B expression were detected. (C) MACS-purified and FACS-sorted ($CD3^-NK1.1^+$) *Stat3*$^{fl/fl}$ and *Stat3*$^{\Delta/\Delta}$*Ncr1*-iCreTg NK cells were stimulated *ex vivo* with IL-2 alone or together with IL-12. *Gzmb* and *Prf1* mRNA expressions were determined by qPCR. Data represent means±SEM of two independent

experiments (n≥5); RNA levels are calculated relative to that of the housekeeping gene (HKG) *Rplp0*. (D+E) Splenocytes from *Stat3*$^{fl/fl}$ and *Stat3*$^{\Delta/\Delta}$*Ncr1*-iCreTg mice were analyzed directly *ex vivo* or after stimulation for 8 hours with IL-2, IL-12 and IL-15 and stained for CD3, NKp46 (CD3$^-$NKp46$^+$) and perforin or granzyme B. Levels were analyzed by flow cytometry. Bar graphs depict mean fluorescence intensities (MFI) (n≥7 per genotype). (F) MACS-purified and FACS-sorted (CD3$^-$NK1.1$^+$) NK cells were treated with DMSO (control), with 0.5, 5, 10 or 20µM of the STAT3 inhibitor LLL-12 or with 100µM of the STAT3 inhibitor S3I-201 for 4 hours. NK cells were either left untreated (IL-2 media only) or stimulated with IL-12 for 20 minutes. Western blot analysis shows levels of pSTAT3-Y705 and STAT3. ß-actin was used as loading control. (G) MACS-purified and FACS-sorted (CD3-NK1.1$^+$) NK cells were treated with DMSO, with 0.5µM of the inhibitor LLL-12 or with 100µM of the inhibitor S3I-201 for 4 hours following stimulation with IL-2, IL-2+IL-12 or IL-2+IL-12+IL-15 for 3 hours. Perforin and granzyme B mRNA levels were analyzed by qPCR. (Data represent means±SEM; Levels are calculated relative to the housekeeping gene (HKG) *Rplp0*.

Figure 4: **STAT3 regulates NK cell-dependent IFN-γ production by directly binding to the IFN-γ promoter**. (A) Splenocytes from *Stat3*$^{fl/fl}$ and *Stat3*$^{\Delta/\Delta}$*Ncr1*-iCreTg mice were analyzed directly *ex vivo* or after 4 hours stimulation with IL-2+IL-12. Cells were stained for CD3 and NKp46 (CD3$^-$NKp46$^+$) followed by fixation, permeabilization and intracellular staining of T-bet and IFN-γ. Levels were analyzed by flow cytometry. % IFN-γ$^+$ NK cells and mean fluorescence intensities (MFI) of T-bet are depicted in representative FACS plots. Statistics are included in Figure S4D. (B) Splenocytes from *Stat3*$^{fl/fl}$ and *Stat3*$^{\Delta/\Delta}$*Ncr1*-iCreTg mice were analyzed directly *ex vivo* or after stimulation for 4 or 8 hours with IL-2+IL-12. Intracellular IFN-γ expression of NK cells were analyzed by flow cytometry. *Stat3*$^{\Delta/\Delta}$*Ncr1*-iCreTg NK cells show a decreased IFN-γ production after 4 hours that is no longer detectable after 8 hours. Data represent means ± SEM

of 3 independent experiments (n≥13 in total). (C) Primary IL-2 cultured NK cells were stimulated for 30 minutes with IL-2 or IL-2+IL-12. The reaction was stopped by addition of formaldehyde. Chromatin Immunoprecipitation was performed using an anti-STAT3 antibody and n-fold-enrichment was calculated relative to the expression of a negative region ("CD19 down"). (D) NK cells of *Stat3*$^{fl/fl}$ and *Stat3*$^{\Delta/\Delta}$*Ncr1*-iCreTg mice were MACS-purified and FACS-sorted (CD3$^-$ NK1.1$^+$) and stimulated with IL-2 and IL-12 for the indicated length of time. Cell lysates were used for western blot analysis of pSTAT5-Y694, STAT5a/b, STAT3, pSTAT4-Y693 and STAT4. ß-actin was used as loading control. *Stat3*$^{\Delta/\Delta}$*Ncr1*-iCreTg NK cells show an increase in STAT4 and STAT5 activation compared to *Stat3*$^{fl/fl}$ controls. (E) Splenocytes from *Stat3*$^{fl/fl}$ and *Stat3*$^{\Delta/\Delta}$*Ncr1*-iCreTg mice were stimulated with anti-NK1.1 (PK136) for 4 or 8 hours prior to staining for CD3 and NKp46 (CD3$^-$NKp46$^+$) followed by fixation, permeabilization and intracellular staining and detection of IFN-γ expression by flow cytometry. (F) Splenocytes from *Stat3*$^{fl/fl}$ and *Stat3*$^{\Delta/\Delta}$*Ncr1*-iCreTg mice were stimulated with anti-NK1.1 (PK136) for 6 hours prior to staining for CD3, NKp46 and Ly49C/I. Cells were fixed, permeabilized and intracellular IFN-γ expression of the Ly49C negative and positive NK cell fraction (CD3$^-$NKp46$^+$ cells) was analyzed. Statistics are included in Figure S4A.

Figure 5: ***Stat3*-deficient NK cells show enhanced *in vitro* cytotoxicity against B16F10 melanoma cells.** (A+B) 5x10^4 B16F10 melanoma cells were injected i.v. into *Stat3*$^{fl/fl}$, *Stat3*$^{\Delta/\Delta}$*Ncr1*-iCreTg, *Ncr1*-iCreTg and wild-type mice. After 24 days the number of tumor nodules in the lung was assessed by 3 independent researchers in a blinded manner. (B) Statistical analysis summarizes 4 independent experiments (n≥11 in total). (C) DNAM-1 expression on *Stat3*$^{fl/fl}$ (n=11) and *Stat3*$^{\Delta/\Delta}$*Ncr1*-iCreTg (n=10) NK cells in the blood of B16F10 inoculated mice was analyzed twice a week using flow cytometry (gated on CD3$^-$NKp46$^+$NK

cells). Graph represents means±SEM. (D) *In vitro* cytotoxicity assays of IL-2-cultured NK cells with RMA, RMA-Rae1, YAC-1, *v-abl*$^+$ and B16F10 target cell lines. The effector:target (E:T) cell ratios ranged from 1:1 to 10:1. After 4-6 hours incubation at 37°C lysis of targets cells was analyzed by flow cytometry. Graphs represent means±SEM (biological replicates: 2, technical replicates: 3 each). (E) RMA, RMA-Rae1, YAC-1, *v-abl*$^+$ cell line #1 and cell line #2 and B16F10 target cell lines were analyzed for the expression of the DNAM-1 ligand CD155 by flow cytometry. (F) IL-2-cultured *Stat3*$^{fl/fl}$ and *Stat3*$^{\Delta/\Delta}$*Ncr1*-iCreTg NK cells were treated with an anti-DNAM-1 antibody for 1 hour. Control and DNAM-1-blocked NK cells of both genotypes were incubated with B16F10 target cells. The effector:target (E:T) cell ratios ranged from 1:1 to 7.5:1 and after 4 hours incubation on 37°C the lysis of the targets cells was analyzed by flow cytometry. Symbols represent means and error bars indicate SEM of triplicates. Data are representative for 2 independent experiments.

Figure 6: ***Stat3*$^{\Delta/\Delta}$*Ncr1*-iCreTg mice show enhanced tumor surveillance in leukemia and lymphoma models *in vivo***. (A+B) 10^6 *v-abl*$^+$ leukemic cells were injected s.c. in the flanks of *Stat3*$^{fl/fl}$ and *Stat3*$^{\Delta/\Delta}$*Ncr1*-iCreTg mice. After 12 days tumor weight was determined (A). (B) Bar graphs summarize data of 3 independent experiments with n≥14. (C) Kaplan-Meier plot of *Stat3*$^{fl/fl}$ (n=7) and *Stat3*$^{\Delta/\Delta}$*Ncr1*-iCreTg (n=9) mice after i.v. injection of 10^6 *v-abl*$^+$ leukemic cells. One representative of 2 independent experiments is shown. Mice were sacrificed at the first signs of paralysis and poor health. (D) Newborn *Stat3*$^{fl/fl}$ (n=12) and *Stat3*$^{\Delta/\Delta}$*Ncr1*-iCreTg (n=7) mice were infected with a replication-incompetent ecotropic retrovirus encoding for *v-abl* by s.c. injection. Mice were sacrificed at first signs of paralysis and health detractions. One representative of 3 independent experiments is shown. (E) H&E stains of blood and bone marrow of *Stat3*$^{fl/fl}$ and *Stat3*$^{\Delta/\Delta}$*Ncr1*-iCreTg mice suffering from *v-abl* induced leukemia.

Figure 1

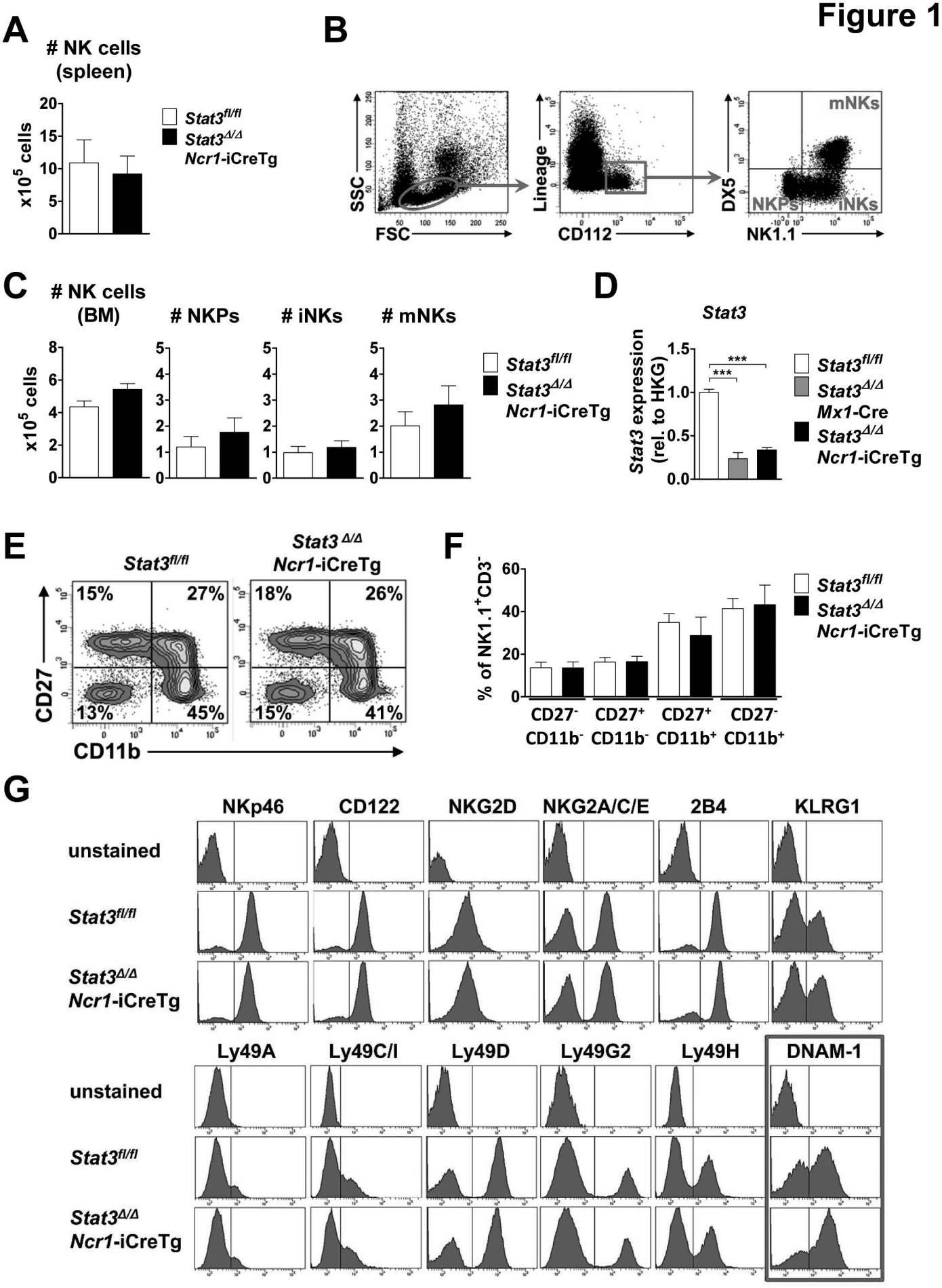
A
NK cells (spleen)
x10^5 cells
Stat3^fl/fl
Stat3^Δ/Δ Ncr1-iCreTg
B
SSC
FSC
Lineage
CD112
DX5
NK1.1
mNKs
NKPs
iNKs
C
NK cells (BM)
NKPs
iNKs
mNKs
x10^5 cells
Stat3^fl/fl
Stat3^Δ/Δ Ncr1-iCreTg
D
Stat3
Stat3 expression (rel. to HKG)
***
***
Stat3^fl/fl
Stat3^Δ/Δ Mx1-Cre
Stat3^Δ/Δ Ncr1-iCreTg
E
Stat3^fl/fl
Stat3^Δ/Δ Ncr1-iCreTg
15%
27%
13%
45%
18%
26%
15%
41%
CD27
CD11b
F
% of NK1.1+CD3-
CD27- CD11b-
CD27+ CD11b-
CD27+ CD11b+
CD27- CD11b+
Stat3^fl/fl
Stat3^Δ/Δ Ncr1-iCreTg
G
NKp46
CD122
NKG2D
NKG2A/C/E
2B4
KLRG1
unstained
Stat3^fl/fl
Stat3^Δ/Δ Ncr1-iCreTg
Ly49A
Ly49C/I
Ly49D
Ly49G2
Ly49H
DNAM-1
unstained
Stat3^fl/fl
Stat3^Δ/Δ Ncr1-iCreTg

Figure 2

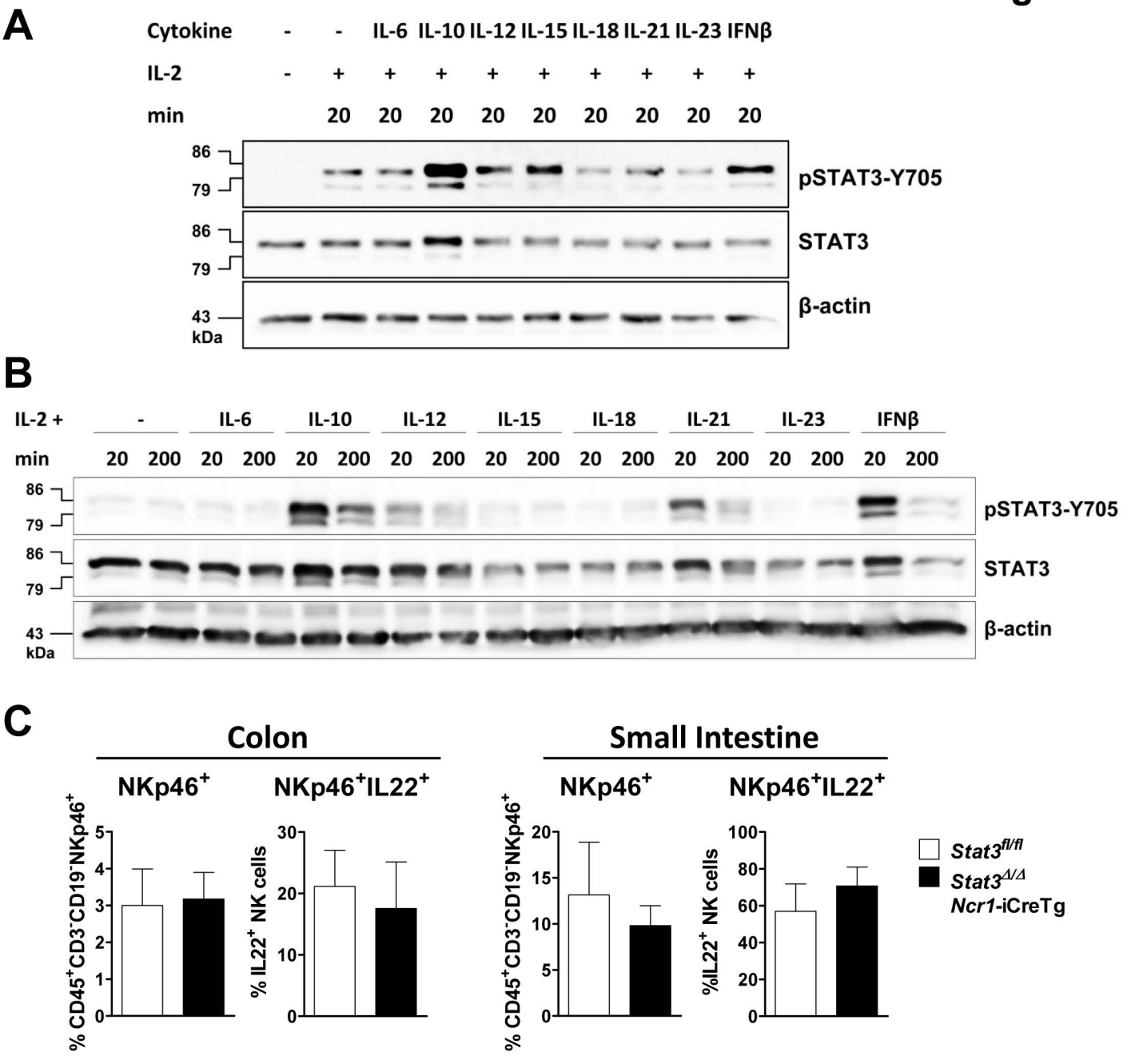
A
Cytokine - - IL-6 IL-10 IL-12 IL-15 IL-18 IL-21 IL-23 IFNβ
IL-2 - + + + + + + + + +
min 20 20 20 20 20 20 20 20 20
86
79
pSTAT3-Y705
86
79
STAT3
43
kDa
β-actin
B
IL-2 + - IL-6 IL-10 IL-12 IL-15 IL-18 IL-21 IL-23 IFNβ
min 20 200 20 200 20 200 20 200 20 200 20 200 20 200 20 200 20 200
86
79
pSTAT3-Y705
86
79
STAT3
43
kDa
β-actin
C
Colon
Small Intestine
NKp46+
NKp46+IL22+
% CD45+CD3-CD19-NKp46+
% IL22+ NK cells
%IL22+ NK cells
Stat3fl/fl
Stat3Δ/Δ
Ncr1-iCreTg

Figure 3

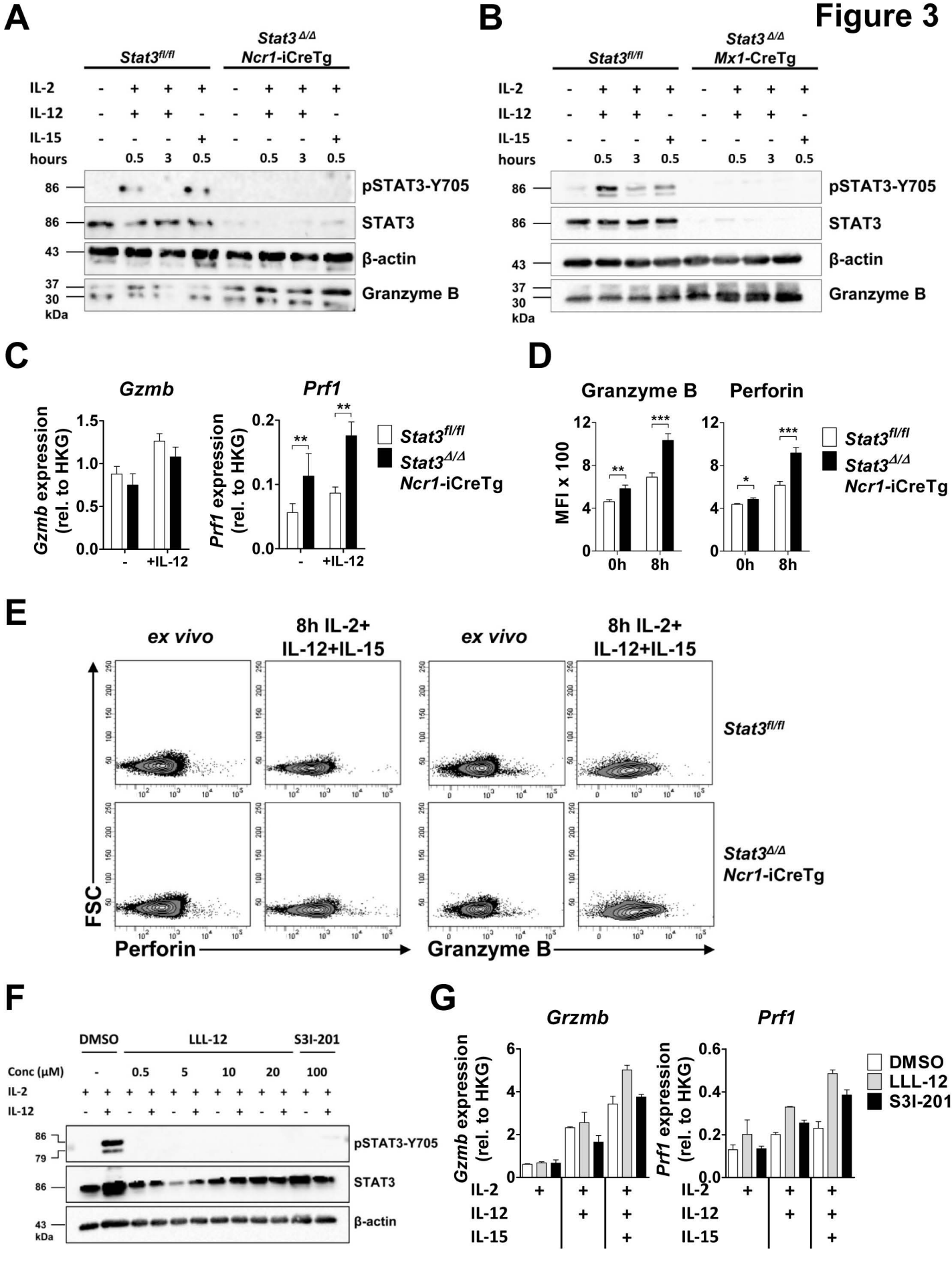
A
Stat3fl/fl
Stat3Δ/Δ Ncr1-iCreTg
IL-2
IL-12
IL-15
hours
0.5 3 0.5 0.5 3 0.5
86
pSTAT3-Y705
86
STAT3
43
β-actin
37
30
kDa
Granzyme B
B
Stat3fl/fl
Stat3Δ/Δ Mx1-CreTg
C
Gzmb
Prf1
Gzmb expression (rel. to HKG)
Prf1 expression (rel. to HKG)
Stat3fl/fl
Stat3Δ/Δ Ncr1-iCreTg
-
+IL-12
D
Granzyme B
Perforin
MFI x 100
0h
8h
E
ex vivo
8h IL-2+ IL-12+IL-15
Stat3fl/fl
Stat3Δ/Δ Ncr1-iCreTg
FSC
Perforin
Granzyme B
F
DMSO
LLL-12
S3I-201
Conc (μM)
pSTAT3-Y705
STAT3
β-actin
G
Grzmb
Prf1
DMSO
LLL-12
S3I-201

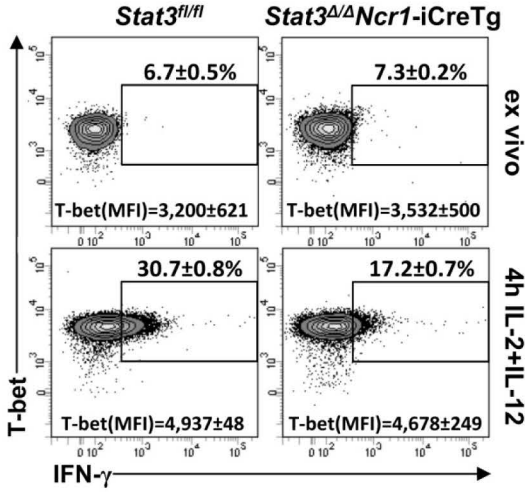
A
Stat3fl/fl
Stat3Δ/ΔNcr1-iCreTg
6.7±0.5%
7.3±0.2%
ex vivo
T-bet(MFI)=3,200±621
T-bet(MFI)=3,532±500
30.7±0.8%
17.2±0.7%
4h IL-2+IL-12
T-bet(MFI)=4,937±48
T-bet(MFI)=4,678±249
T-bet
IFN-γ

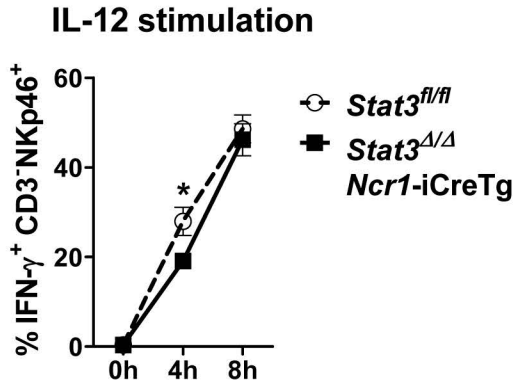
B
IL-12 stimulation
% IFN-γ+ CD3-NKp46+
Stat3fl/fl
Stat3Δ/Δ
Ncr1-iCreTg
0h
4h
8h

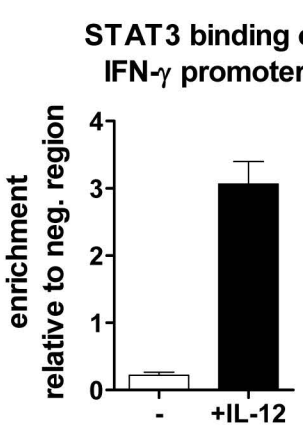
C
STAT3 binding on
IFN-γ promoter
enrichment
relative to neg. region
-
+IL-12

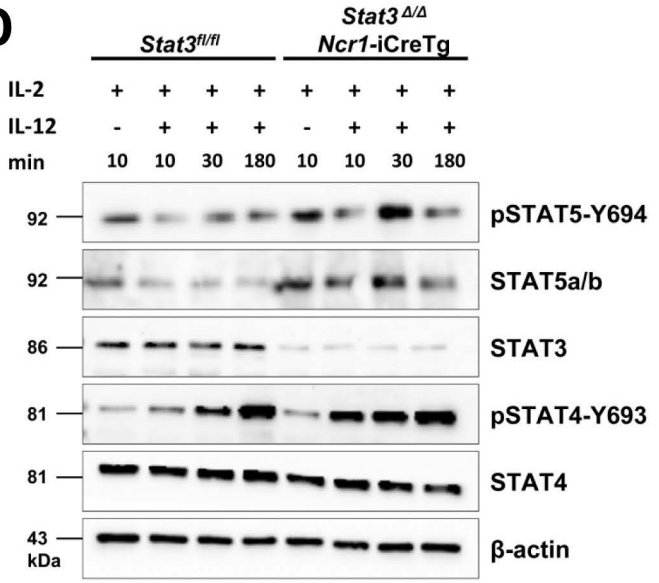
D
Stat3fl/fl
Stat3Δ/Δ
Ncr1-iCreTg
IL-2
IL-12
min
92
pSTAT5-Y694
92
STAT5a/b
86
STAT3
81
pSTAT4-Y693
81
STAT4
43
kDa
β-actin

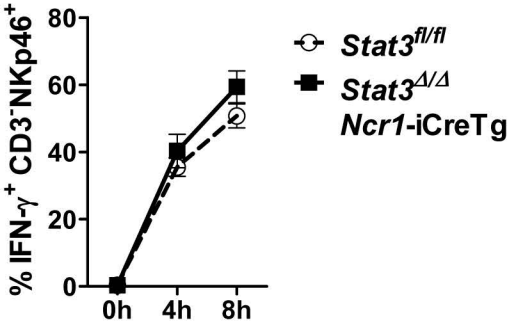
E
NK1.1 receptor activation
% IFN-γ+ CD3-NKp46+
Stat3fl/fl
Stat3Δ/Δ
Ncr1-iCreTg
0h
4h
8h

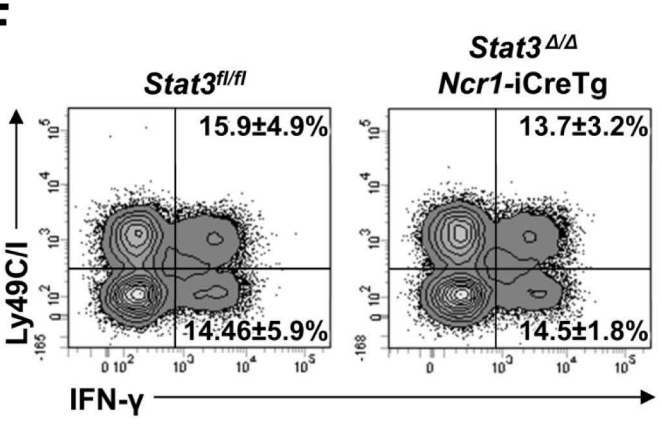
F
Stat3fl/fl
Stat3Δ/Δ
Ncr1-iCreTg
15.9±4.9%
13.7±3.2%
14.46±5.9%
14.5±1.8%
Ly49C/I
IFN-γ

Figure 5

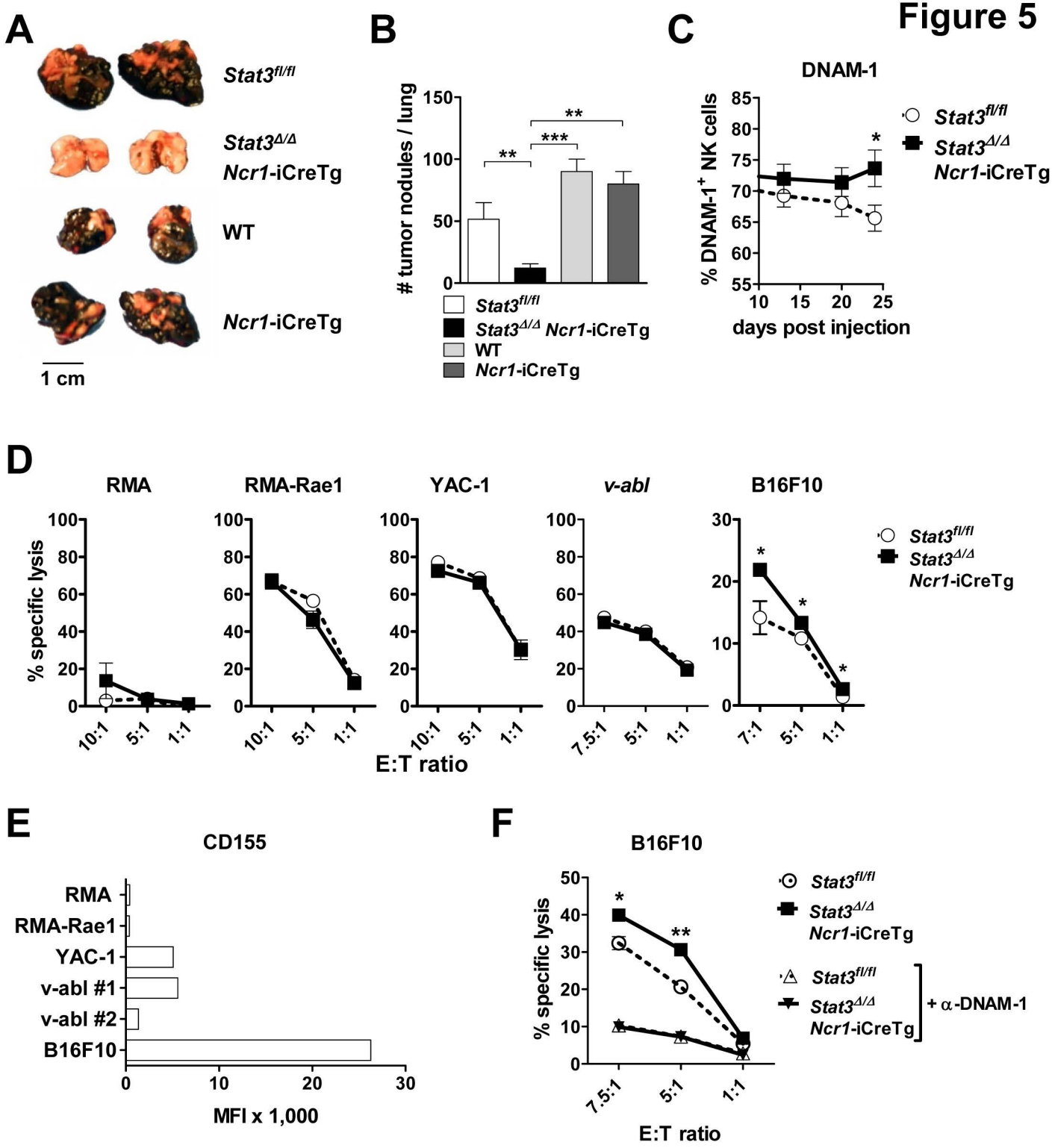
A
Stat3fl/fl
Stat3Δ/Δ Ncr1-iCreTg
WT
Ncr1-iCreTg
1 cm
B
tumor nodules / lung
150
100
50
0
**
***
**
Stat3fl/fl
Stat3Δ/Δ Ncr1-iCreTg
WT
Ncr1-iCreTg
C
DNAM-1
% DNAM-1+ NK cells
85
80
75
70
65
60
55
10 15 20 25
days post injection
*
Stat3fl/fl
Stat3Δ/Δ Ncr1-iCreTg
D
RMA
RMA-Rae1
YAC-1
v-abl
B16F10
% specific lysis
100
80
60
40
20
0
30
20
10
10:1 5:1 1:1
7.5:1 5:1 1:1
7:1 5:1 1:1
E:T ratio
Stat3fl/fl
Stat3Δ/Δ Ncr1-iCreTg
E
CD155
RMA
RMA-Rae1
YAC-1
v-abl #1
v-abl #2
B16F10
0 10 20 30
MFI x 1,000
F
B16F10
% specific lysis
50
40
30
20
10
0
7.5:1 5:1 1:1
E:T ratio
Stat3fl/fl
Stat3Δ/Δ Ncr1-iCreTg
Stat3fl/fl
Stat3Δ/Δ Ncr1-iCreTg
+ α-DNAM-1

Figure 6

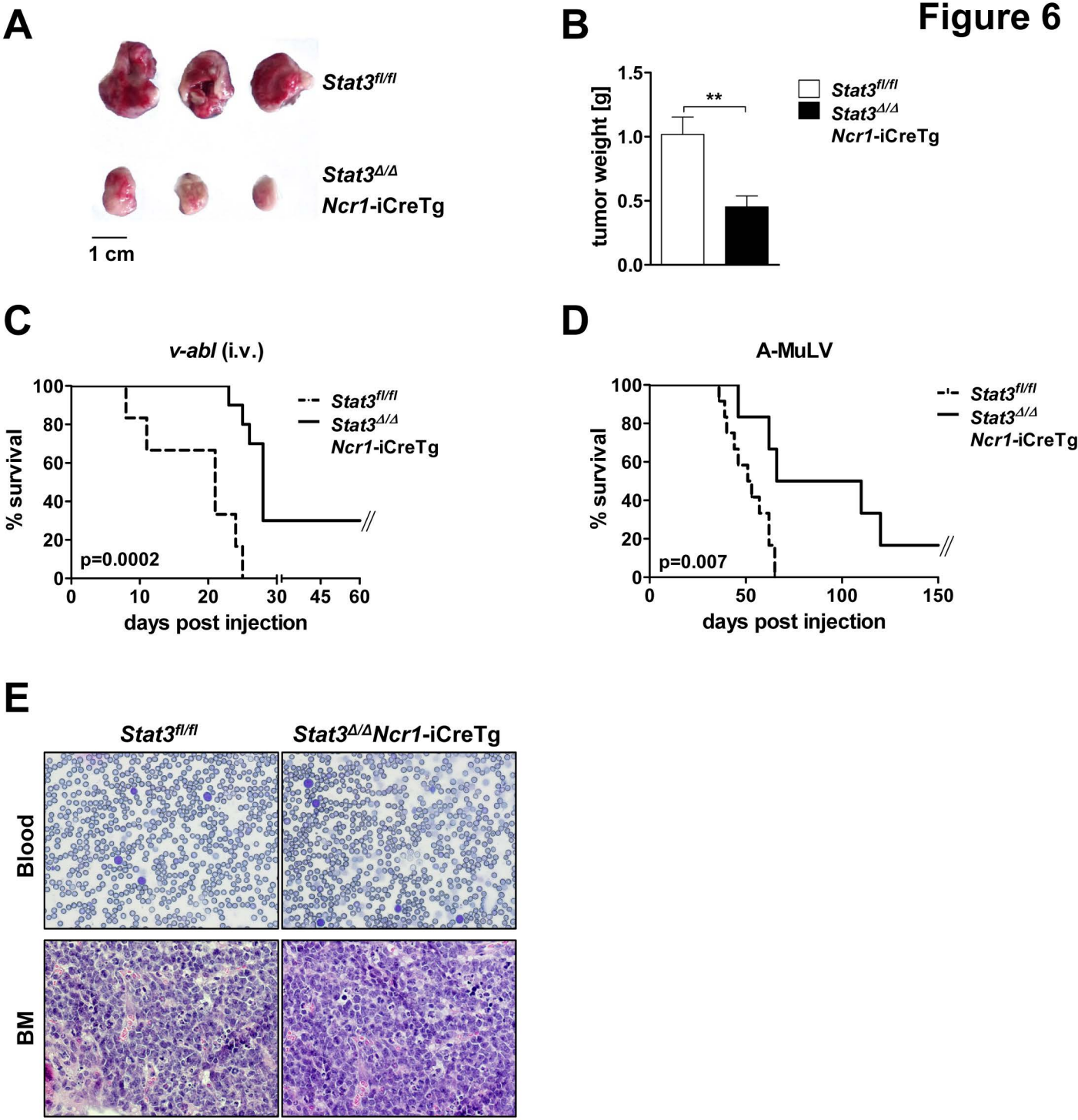
A
Stat3fl/fl
Stat3Δ/Δ
Ncr1-iCreTg
1 cm
B
tumor weight [g]
1.5
1.0
0.5
0.0
**
Stat3fl/fl
Stat3Δ/Δ
Ncr1-iCreTg
C
v-abl (i.v.)
% survival
100
80
60
40
20
0
p=0.0002
0
10
20
30
45
60
days post injection
Stat3fl/fl
Stat3Δ/Δ
Ncr1-iCreTg
D
A-MuLV
% survival
100
80
60
40
20
0
p=0.007
0
50
100
150
days post injection
Stat3fl/fl
Stat3Δ/Δ
Ncr1-iCreTg
E
Stat3fl/fl
Stat3Δ/ΔNcr1-iCreTg
Blood
BM